

G protein-coupled receptor 183 facilitates endothelial-to-hematopoietic transition via Notch1 inhibition

Panpan Zhang¹, Qiuping He¹, Dongbo Chen², Weixiao Liu³, Lu Wang¹, Chunxia Zhang¹, Dongyuan Ma¹, Wei Li³, Bing Liu², Feng Liu¹

¹State Key Laboratory of Membrane Biology, Institute of Zoology, Chinese Academy of Sciences, Beijing 100101, China; ²307-Ivy Translational Medicine Center, Laboratory of Oncology, Affiliated Hospital of Academy of Military Medical Sciences, Beijing 100071, China; ³State Key Laboratory of Reproductive Biology, Institute of Zoology, Chinese Academy of Sciences, Beijing 100101, China

In vertebrates, embryonic hematopoietic stem and progenitor cells (HSPCs) are derived from a subset of endothelial cells, the hemogenic endothelium (HE), through the endothelial-to-hematopoietic transition (EHT). Notch signaling is essential for HSPC development during embryogenesis across vertebrates. However, whether and how it regulates EHT remains unclear. Here, we show that G protein-coupled receptor 183 (Gpr183) signaling serves as an indispensable switch for HSPC emergence by repressing Notch signaling before the onset of EHT. Inhibition of Gpr183 significantly upregulates Notch signaling and abolishes HSPC emergence. Upon activation by its ligand 7 α -25-OHC, Gpr183 recruits β -arrestin1 and the E3 ligase Nedd4 to degrade Notch1 in specified HE cells and then facilitates the subsequent EHT. Importantly, 7 α -25-OHC stimulation promotes HSPC emergence *in vivo* and *in vitro*, providing an attractive strategy for enhancing the *in vitro* generation of functional HSPCs.

Keywords: hematopoietic stem and progenitor cell; hemogenic endothelium; endothelial-to-hematopoietic transition; Gpr183; Notch1; Nedd4; 7 α -25-OHC

Cell Research (2015) 25:1093-1107. doi:10.1038/cr.2015.109; published online 11 September 2015

Introduction

Hematopoietic stem cells (HSCs) produce all lineages of blood cells and maintain lifelong hematopoiesis in vertebrates. Although HSC transplantation is used to treat hematopoietic malignancies including leukemia, its application has been limited mainly due to the severe shortage of compatible donors to supply functional hematopoietic stem and progenitor cells (HSPCs). Therefore, understanding the mechanism underlying HSC or HSPC generation and development is of great clinical importance for regenerative medicine. Previous studies have demonstrated that embryonic HSPCs in vertebrates are generated from a group of specialized endothelial cells, named hemogenic endothelium (HE) [1-4], through

the endothelial-to-hematopoietic transition (EHT) [5-7]. Several important regulators or signaling pathways have been identified as playing roles in this process [8-10]. However, how these intrinsic and extrinsic regulators and signaling pathways spatially and temporally regulate the development of HSPCs from hemogenic endothelial cells (HECs) still remains elusive.

Notch signaling is an important and conserved signaling pathway during embryogenesis, particularly neurogenesis and cardiovascular development. Previous studies revealed that Notch signaling is indispensable for embryonic HE specification [11], as well as artery development [12, 13], and the function of Notch signaling in promoting definitive haematopoiesis could be uncoupled from that in artery development [11, 14]. However, recent studies reported that elevated levels of Notch signaling impede HSPC generation in chick and mouse embryos [15, 16], suggesting unexpected complexities in the role of Notch signaling during hematopoiesis.

G protein-coupled receptors (GPCRs) constitute the largest receptor family; they are involved in a variety

Corresponding authors: Feng Liu

Tel: +86-10-64807307; Fax: +86-10-64807313

E-mail: liuf@ioz.ac.cn

Received 23 July 2015; revised 28 July 2015; accepted 31 July 2015; published online 11 September 2015

of physiological processes. In most cases, GPCRs are responsible for sensing external signals including odors, taste, neurotransmitters or inflammation signals [17]. The contribution of GPCRs to embryonic hematopoiesis has only recently been realized. Thrombin receptor (*f2r*) inhibits EHT by interacting with RhoA/ROCK signaling [18]. Prostaglandin E2 (PGE2), which signals through a GPCR, can expand HSPC population [19]. Moreover, *Gpr56* is highly enriched in hematopoietic clusters and is essential for HSPC generation [20]. However, how GPCR signaling is integrated with other hematopoiesis-related signaling pathways during embryonic HSPC development is still poorly characterized.

Here, we report a novel regulator of HSPC development: GPCR *gpr183*, identified through a transcriptome analysis using a newly generated Tg(*runx1:en-GFP*) line. Functional analysis indicates that *gpr183* is indispensable for HSPC emergence but not HE specification in both zebrafish and mouse. Unexpectedly, we find that Notch signaling is not continuously required during HSPC development: after HE specification, Notch signaling is downregulated to allow HSPC emergence. The downregulation of Notch signaling requires *Gpr183*, which, upon activation by its endogenous ligand 7 α -25-OHC, recruits β -arrestin1 (*Arrb1*) and E3 ligase *Nedd4* to degrade Notch1 receptor in HE, thus facilitating the transition from endothelial to hematopoietic lineage. Importantly, activation of the *Gpr183*-*Arrb1*-Notch1 signaling cascade can promote HSPC development in both zebrafish and mouse, suggesting conservation of this mechanism and potential therapeutic value of *Gpr183* ligands in regenerative medicine.

Results

Establishment of Tg(runx1:en-GFP) line and RNA sequencing

Using a mouse *runx1*+24 enhancer [21], we generated a new zebrafish transgenic line Tg(*runx1:en-GFP*) that recapitulated *runx1* endogenous expression during HE specification and HSPC emergence (Figure 1A, Supplementary information, Figure S1A, S1B and Movie S1). *runx1* knockdown greatly attenuated the population of GFP⁺ cells in the aorta-gonad-mesonephros (AGM), the caudal hematopoietic tissue (CHT) and the thymus (Supplementary information, Figure S1B), supporting the notion that these GFP⁺ cells are *runx1*-dependent HSPCs [22]. To explore the mechanism governing HE specification and transformation into HSPCs through EHT, non-hemogenic endothelial cells (ECs, *flk1*⁺*runx1*⁻), specified HECs (*flk1*⁺*runx1*⁺), and potential HSPCs (*flk1*⁻*runx1*⁺) were sorted from Tg(*flk1:mCherry/runx-*

1:en-GFP) embryos at 28 h post fertilization (hpf; before the emergence of HSPCs) for RNA deep sequencing analysis (Figure 1A and 1B). RNA-Seq analysis showed a number of differentially expressed genes between two populations in three pairwise comparisons (Figure 1C). Compared with the EC population, many genes known to be involved in hematopoiesis were enriched in HEC or HSPC population, validating reliability of the RNA-Seq data (Supplementary information, Figure S1C and Table S1, RPKM > 2). Heatmap analysis revealed a number of genes highly expressed in HE or HSPC population but were previously less characterized in the context of hematopoiesis (Figure 1D). Expression profile screening by whole mount *in situ* hybridization confirmed that most of these genes were expressed in the AGM region (Supplementary information, Figure S2A). To functionally test these genes, we designed antisense morpholinos (MOs) targeting 11 different genes for knockdown experiments. After knockdown of seven genes, expression of HSPC markers *runx1* and *cmyb* was severely attenuated at 36 hpf (Supplementary information, Figure S2B and S2C), indicating their important roles in definitive hematopoiesis. To determine the conservation of these genes during HE development across species, we compared zebrafish dataset with embryonic day 10.5 (E10.5) mouse HE sequencing results (data not shown) and found that *gpr183* was the most enriched gene in both species.

Gpr183 is essential for HSPC emergence

Gpr183, also called Epstein-Barr virus-induced gene 2 or EBI2, is known for its role in guiding follicular B cell migration after activation by its endogenous ligand, 7-25-OHC [23-25]. However, it was unknown whether and how *gpr183* is involved in HSPC development. The expression profile showed that *gpr183* is expressed in the zebrafish AGM region starting at 26 hpf (Supplementary information, Figure S3A and S3B). Moreover, heatmap analysis confirmed that *gpr183* is highly enriched in the HE population (Figure 1D), which was verified by the qPCR results in sorted ECs, HECs and HSPCs (Supplementary information, Figure S3C). Double fluorescence *in situ* hybridization using 30 hpf Tg(*fli1a:eGFP*) embryos confirmed that *gpr183* is expressed in some endothelial cells in the AGM region (Supplementary information, Figure S3D).

To determine the function of *gpr183* in zebrafish, we generated a *gpr183*-null mutant by removing 11 base pairs in the second exon (292 base pairs after the start codon) using the CRISPR/Cas9 technique (Figure 2A and Supplementary information, Figure S3E). We found that both *cmyb* expression at 36 hpf and T lymphocyte marker *rag1* expression at 5 days post fertilization (dpf)

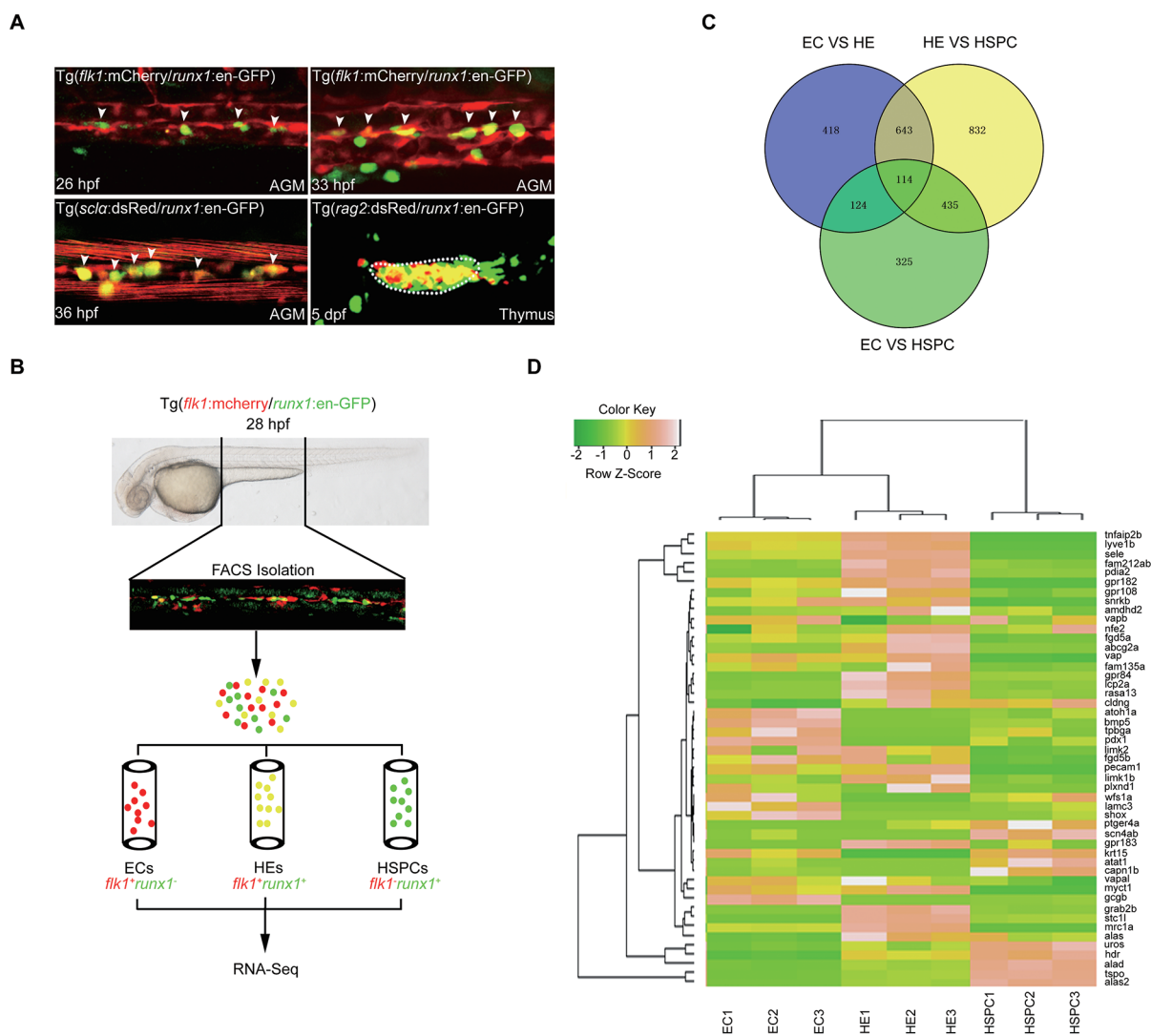


Figure 1 RNA-deep sequencing analysis of gene expression in ECs, HE and HSPCs from Tg(*flk1:mCherry/runx1:en-GFP*) transgenic embryos. **(A)** Fluorescence signals in AGM and thymus of the indicated transgenic lines showing that Tg(*runx1:en-GFP*) is able to label HE and HSPCs. White arrowheads denote HE or emerging HSPCs in AGM. **(B)** Flowchart of sorting and RNA-Seq analysis of the indicated cells from 28 hpf Tg(*flk1:mCherry/runx1:en-GFP*) embryos. **(C)** RNA-Seq analysis results showing the numbers of differentially expressed genes in sorted ECs, HECs and HSPCs from 28 hpf Tg(*flk1:mCherry/runx1:en-GFP*) embryos. **(D)** Heat-map analysis of selected genes based on RNA-Seq data.

were significantly downregulated in *gpr183* mutant (Figure 2B). *7α-25-OHC* is synthesized by Ch25h and Cyp7b1 sequentially *in vivo* [26, 27]. Clotrimazole, an inhibitor of Cyp7b1 [26], was used to block *7α-25-OHC* synthesis, and this treatment effectively attenuated *runx1* expression in AGM and *rag1* expression in thymus (Figure 2C). After crossing *gpr183* mutant with the Tg(*flk1:mCherry/runx1:en-GFP*) reporter line, we found that the HEC population at 36 hpf was significantly disrupted in the absence of *gpr183* signaling (Figure 2D and 2E). Moreover, *gpr183* deficiency also attenuated

EHT (Supplementary information, Movie S2). Kidney marrow, or head kidney, is a hematopoietic organ in adult zebrafish. We found that in 12-week-old *gpr183^{+/-}* adult fish (*gpr183^{-/-}* adult fish were not viable), both the cell number in the head kidney and size of the organ were significantly reduced (Figure 2F), suggesting a defect in definitive hematopoiesis upon *gpr183* haploinsufficiency. Furthermore, time course experiments in *gpr183* mutant and clotrimazole treatment revealed that *gpr183* was not required before HE specification (Supplementary information, Figure S4A-S4D). Taken together, these results

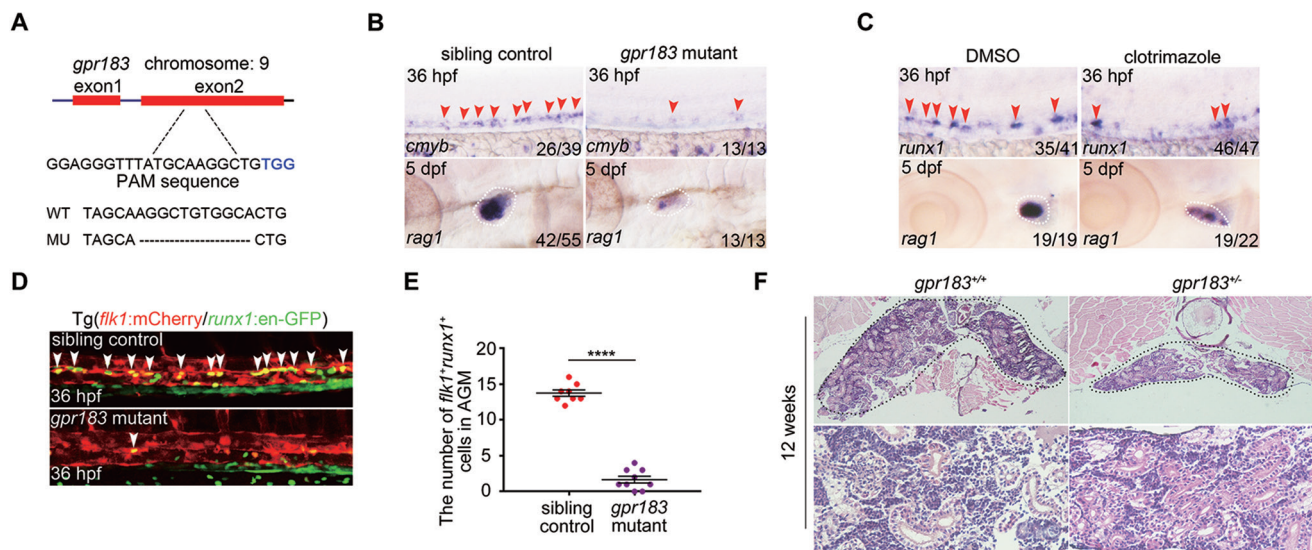


Figure 2 *Gpr183* plays an indispensable role during definitive hematopoiesis in zebrafish. **(A)** Generation of *gpr183* mutant using the CRISPR/Cas9 technique. PAM sequence is ‘TGG’ (in blue); alignment of WT and mutated sequences is listed below. **(B, C)** Reduced expression of *cmyb* (or *runx1*) and *rag1* in *gpr183* mutant embryos **(B)** and clotrimazole-treated embryos **(C)**. Red arrowheads indicate *cmyb* or *runx1* expression in AGM, and white circles denote *rag1* expression in the thymus. **(D)** The number of HE in Tg(*gpr183*^{-/-};*flk1*:mCherry/*runx1*:en-GFP) embryos is attenuated significantly compared with that in control embryos. White arrowheads denote HE in the AGM region. **(E)** Dot-plot quantification analysis of HE in sibling control and *gpr183* mutant. Error bar represents SD. *****P* < 0.0001. **(F)** Hematoxylin-eosin staining of head kidney section showing hematopoietic defect in 12-week-old *gpr183* heterozygous mutant fish.

indicate that *Gpr183* is required for HSPC development in zebrafish.

Gpr183 specifically appears to regulate HSPC emergence. We did not observe any general developmental defects, or abnormality in HSPC niche, or aberration in cell proliferation and apoptosis in *gpr183* morphants or mutant (Supplementary information, Figure S5A-S5D).

Notch signaling is downstream of *Gpr183*

We noticed that expression level of arterial marker *ephrinB2a* was increased in embryos treated with clotrimazole (Supplementary information, Figure S6A). Because *ephrinB2a* is a Notch target, we wondered whether Notch signaling is involved in the regulation of HSPC emergence by *Gpr183*. We thus examined another Notch target gene *hey2* and found that its expression was significantly increased upon *gpr183* signaling inhibition from 33 hpf (Figure 3A and Supplementary information, Figure S6B). DBZ, a Notch signaling inhibitor, reversed *cmyb* and *hey2* phenotype in *gpr183*^{-/-} embryos (Figure 3A-3C). Moreover, the upregulation of Notch target genes including *ephrinB2*, *hey2*, *her6*, and *her9* and downregulation of *cmyb* in clotrimazole-treated embryos were also reversed by DBZ treatment (Supplementary information, Figure S6A-S6D). These data together sug-

gest that Notch signaling acts downstream of *Gpr183*. To define whether *Gpr183* modulates Notch signaling in a cell-autonomous manner, we treated Tg(*flk1*:mCherry/*runx1*:en-GFP) embryos with DMSO or clotrimazole and sorted the *flk1*⁺*runx1*⁻ and *flk1*⁺*runx1*⁺ cells at 28 hpf for qPCR analysis. Expression levels of Notch target genes *her6* and *her9* increased remarkably in the *flk1*⁺*runx1*⁺ cells (HECs) but not in the *flk1*⁺*runx1*⁻ cells (non-hemogenic ECs) after clotrimazole treatment compared with the DMSO control (Figure 3D), supporting that *Gpr183* modulates Notch signaling in HE in a cell-autonomous manner.

Notch signaling downregulation is required for HSPC development

Previous findings have demonstrated that Notch signaling is indispensable for definitive hematopoiesis, whereas some recent studies have also suggested that activated Notch signaling impedes HSPC development [15, 28]. Our study provides several lines of evidence that suggest that Notch signaling is not continuously required during HSPC development, and downregulation of Notch signaling is a prerequisite for HSPC emergence. First, *fli1*⁺*tp1*⁺ cells in Tg(*fli1a*:eGFP/*tp1*:mCherry) embryos (*tp1*:mCherry is a Notch reporter) were significantly in-

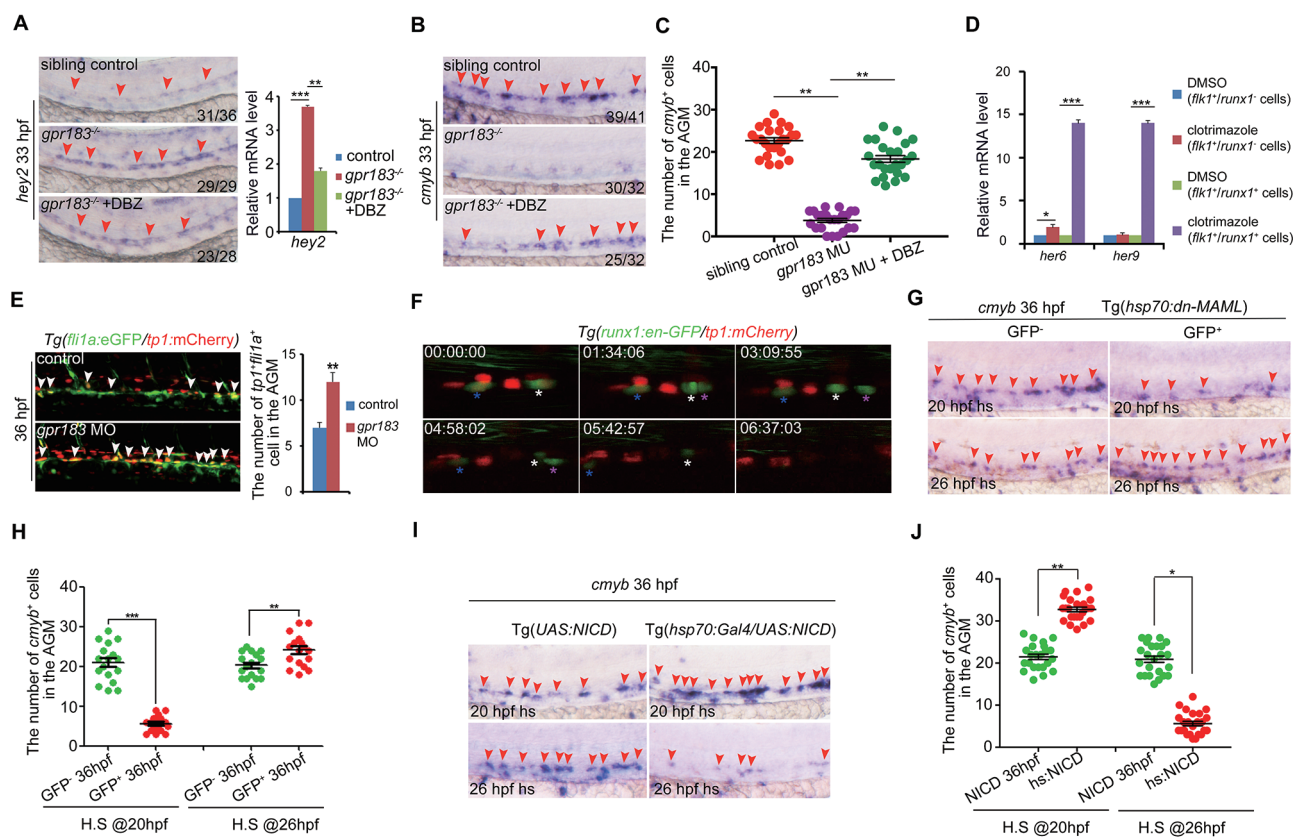


Figure 3 Downregulation of Notch signaling is required for definitive hematopoiesis. **(A)** The increase in *hey2* expression in *gpr183* mutant is reversed by DBZ treatment. Right panel shows the qPCR quantification. **(B)** The decrease in *cmyb* expression in *gpr183* mutant is reversed by DBZ treatment. In **A** and **B**, red arrowheads indicate *hey2* or *cmyb* expression in the AGM region at 33 hpf. **(C)** Dot-plot analysis of *cmyb*⁺ cell numbers in AGM. **(D)** Clotrimazole treatment increases expression levels of *her6* and *her9* in *flk1*⁺*runx1*⁺ cells at 28 hpf. **(E)** Notch-active endothelial cells increase in *gpr183* morphant ($n = 15$ for control and morpholino treatment). Right panel shows the quantification analysis. **(F)** EHT from 37 (shown as 00:00:00) to 43 hpf in *Tg(runx1:en-GFP/tp1:mCherry)* embryo. Asterisks label individual cells. **(G, H)** *cmyb* expression in the AGM region of control embryos and embryos in which Notch signaling is inhibited. *Tg(hsp70:dn-MAML)* embryos expressing a dominant negative (*dn*) isoform of the murine mastermind-like (MAML) protein fused to GFP under a *hsp70* promoter were heat shocked at 20 or 26 hpf; *cmyb* expression was examined at 36 hpf. GFP⁻ embryo serves as a control. Representative images are shown in **G** and the dot-plot quantification analysis is shown in **H**. **(I, J)** *cmyb* expression in the AGM region of control and Notch signaling-activated embryos. *Tg(UAS:NICD)* (NICD, control) and *Tg(hsp70:GAL4/UAS:NICD)* (*hs:NICD*) embryos were heat shocked at 20 or 26 hpf and *cmyb* expression was examined at 36 hpf. Representative images are shown in **I**, and the dot-plot quantification analysis is shown in **J**. In **G** and **I**, red arrowheads mark the staining signals in AGM. Error bar represents SD. * $P < 0.05$, ** $P < 0.01$, *** $P < 0.001$.

creased upon *gpr183* knockdown (Figure 3E). Second, we monitored EHT in *Tg(cmyb:GFP/tp1:mCherry)* or *Tg(runx1:en-GFP/tp1:mCherry)* embryos and found that there were no *tp1*⁺*cmyb*⁺ or *tp1*⁺*runx1*⁺ cells undergoing EHT (even though some emerging cells were initially *runx1*⁺*tp1*⁺, they eventually developed into *runx1*⁺*tp1*⁻ cells; Figure 3F, Supplementary information, Movies S3 and S4).

Moreover, in the transgenic line *Tg(hsp70:dn-MAML)*, which expresses a dominant-negative form of *MAML* (a

transcriptional co-activator for Notch signaling) upon heat shock treatment [29], *cmyb* expression at 36 hpf was significantly lower than the level observed in control embryos when the heat shock treatment was applied at 20 hpf, but was significantly higher than the control when embryos were heat shocked at 26 hpf (Figure 3G and 3H). Finally, in the *Tg(hsp70:GAL4/UAS:NICD)* [30] embryos, which express Notch intracellular domain (NICD) upon heat shock treatment, *cmyb* expression was significantly higher than the level observed in control

embryos (*Tg(UAS:NICD)*) when the heat shock treatment was applied at 20 hpf, but was significantly lower than the control when embryos were heat shocked at 26 hpf (Figure 3I and 3J).

Gpr183 cooperates with Arrb1 to suppress Notch signaling

We next explored the mechanism by which *Gpr183* represses Notch signaling in HE. Previous results have

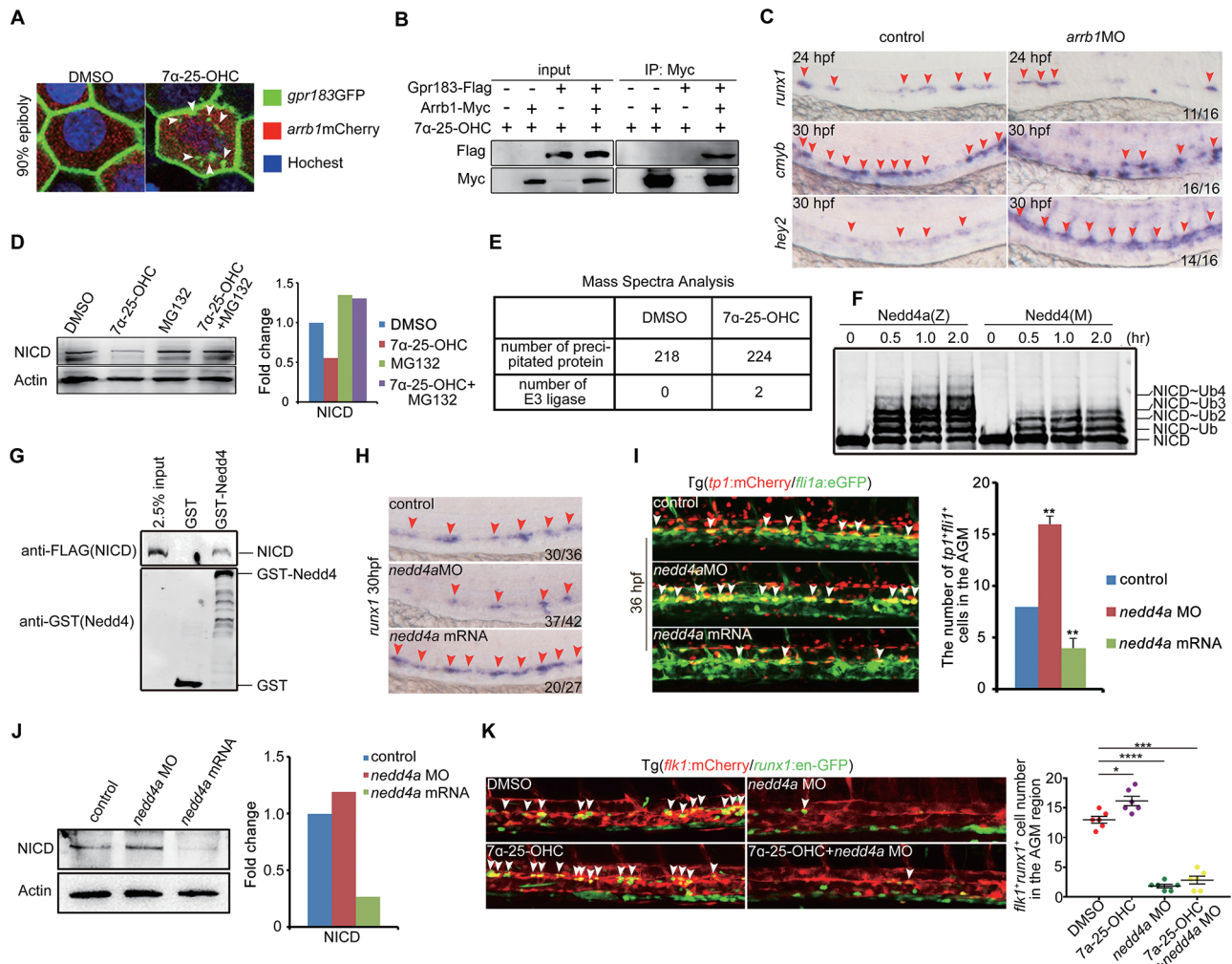


Figure 4 *Gpr183* cooperates with *Arrb1* and *Nedd4* to downregulate Notch signaling. **(A)** Internalization of *Gpr183*-GFP in 90% epiboly embryos ($n = 6$ for each treatment). White arrowheads denote the internalized *Gpr183*-GFP in cytoplasm. **(B)** *Gpr183* interacts with *Arrb1* in 7α -25-OHC-stimulated cells. 293T cells were transfected with *Gpr183*-Flag and/or *Arrb1*-Myc and stimulated with 7α -25-OHC for 0.5 h. Cell lysates were subjected to immunoprecipitation using anti-Myc followed by western blot analysis. **(C)** Expression of *runx1*, *cmyb* and *hey2* in *arrb1* morphants. Red arrowheads label the staining signals in AGM. **(D)** NICD expression in zebrafish embryos treated with 7α -25-OHC (from 1-cell stage to 36 hpf) or MG132 (from 26 to 36 hpf). Right panel shows the quantification analysis. **(E)** MS analysis of Notch1-interacting proteins in control or 7α -25-OHC-treated AGM cells. Mouse E10.5 AGM cells were cultured in the presence of hematopoietic cytokines for three days, and then treated with DMSO or 7α -25-OHC for 1 h. **(F)** Polyubiquitination of NICD-Flag (zebrafish) induced by zebrafish *Nedd4a*-GST (*Nedd4a*(Z)) or mouse *Nedd4*-GST (*Nedd4*(M)). **(G)** GST pull-down assay showing the interaction between *Nedd4*-GST and NICD-Flag. **(H)** *runx1* expression is reduced in *nedd4a* morphants and increased in *nedd4a*-overexpressing embryos. **(I)** *flk1*⁺*tp1*⁺ cells (white arrowheads) are increased in *nedd4a* morphants and are reduced in *nedd4a*-overexpressing embryos. Right panel shows the quantification result. **(J)** NICD expression in *nedd4a* morphants or *nedd4a*-overexpressing embryos. Right panel shows the quantification result. **(K)** HE in *Tg(flk1:mCherry/runx1:en-GFP)* embryos after *nedd4a* knock-down or 7α -25-OHC treatment. White arrowheads indicate HE in the AGM region at 36 hpf. Error bar represents SD. * $P < 0.05$, ** $P < 0.01$, *** $P < 0.001$, **** $P < 0.0001$.

revealed that Arrb1 is responsible for GPCR desensitization and internalization [31], and Arrb1 can be recruited by Gpr183 [24]. To test this interaction in zebrafish, we injected *gpr183-eGFP* and *arrb1-mCherry* mRNA into one-cell stage embryos and observed that the GFP signal at cell membrane was internalized upon 7 α -25-OHC stimulation (Figure 4A). Next, we transfected *gpr183-Flag* and *arrb1-Myc* constructs into 293T cells and found that Flag-tagged Gpr183 was precipitated by anti-Myc in the presence of 7 α -25-OHC (Figure 4B), supporting that Arrb1 is recruited by Gpr183 after Gpr183 activation. To determine the function of Arrb1, we knocked down *arrb1* using antisense morpholino and found that *runx1* expression was normal at 24 hpf, but *cmyb* expression level was decreased at 30 hpf (Figure 4C). In addition, *hey2* expression level was increased in *arrb1* morphants at 30 hpf (Figure 4C), consistent with its increase in *gpr183* mutants (Figure 3A). Taken together, we conclude that Gpr183 cooperates with Arrb1 to downregulate Notch signaling.

Gpr183-Arrb1 complex promotes the degradation of Notch1 through Nedd4-mediated ubiquitination

Because the expression of Notch ligands including *deltC*, *deltD*, *dll4*, and *jagged1* was not altered upon Gpr183 deficiency (data not shown), we asked whether Notch receptors were affected. There are four Notch receptors in vertebrates. Among them, Notch1 is known to regulate artery specification and HE specification [11, 14], while Notch3 is required within the somites to specify HSPCs in a cell non-autonomous manner [32]. Considering that Gpr183 cell-autonomously modulates Notch signaling in HECs, we reasoned that Notch1, but not Notch3, is the target of Gpr183 signaling cascade. To examine if the Gpr183-Arrb1 complex represses Notch1 signaling, we first sorted zebrafish *flk1*⁺*runx1*⁺ cells at 28 hpf and found that *notch1a* and *notch1b* mRNA levels did not increase after clotrimazole treatment (data not shown). We next asked whether the Gpr183-Arrb1 complex regulates Notch1 protein stability. To this end, we treated zebrafish embryos with 7 α -25-OHC and found that expression of NICD at 36 hpf was significantly reduced compared with untreated control embryos, and this reduction was partially reversed by a proteasome inhibitor, MG132 (Figure 4D). Treatment with a lysosome inhibitor chloroquine did not reverse the attenuation of NICD levels after 7 α -25-OHC stimulation (data not shown), suggesting that Notch1 is degraded by a Gpr183 signaling-induced proteasome pathway.

To identify the E3 ligase responsible for Notch1 degradation downstream of Gpr183-Arrb1, we performed mass spectrometry (MS) to identify Notch1-binding pro-

teins using E10.5 mouse AGM cells treated with 7 α -25-OHC (Figure 4E, Supplementary information, Tables S2 and S3). Among hits were two ubiquitin ligases: the HECT domain type E3 ligase Nedd4 and the RING finger domain type E3 ligase Pias3. An *in vitro* ubiquitination assay revealed that Nedd4 facilitated poly-ubiquitination of NICD (Figure 4F). GST pull-down assay further demonstrated a direct interaction between Nedd4 and NICD (Figure 4G). We next examined if Nedd4 modulates Notch1 expression *in vivo*. Indeed, expression of HSPC marker *runx1* in *nedd4a* morphants was significantly reduced, whereas in *nedd4a*-overexpressing embryos, *runx1* expression was markedly increased (Figure 4H). In addition, knockdown of *nedd4a* elevated the *tpl*⁺ signal in endothelial cells (Figure 4I). Moreover, western blot analysis revealed that NICD expression was augmented in *nedd4a* morphants but was reduced in *nedd4a*-overexpressing embryos (Figure 4J), further confirming that *nedd4a* negatively regulates Notch signaling *in vivo*. We also observed that the increase in HEC numbers induced by 7-25-OHC treatment could be disrupted by *nedd4a* knockdown (Figure 4K). All these results together indicate that Nedd4 functions downstream of Gpr183 to attenuate Notch activity.

To address the cellular mechanism by which Notch signaling represses HSPC development, we examined the expression of tight junction gene *ve-cadherin* and found an upregulation of *ve-cadherin* upon inhibition of *gpr183* signaling (Figure 5A). Moreover, a large proportion of *cmyb*-GFP positive cells (potential HSPCs) were converted to non-hemogenic ECs after clotrimazole treatment beginning at 30 hpf (Figure 5B, 5C and Supplementary information, Figure S7A). Based on these results and the observation that expression levels of arterial markers are elevated in the absence of *gpr183* signaling (Figure 3A, Supplementary information, Figure S6A and S6B), we speculate that when Notch signaling is activated, the specified HE lose their hematopoietic potential and instead, maintain their arterial fate [33].

7 α -25-OHC treatment facilitates HSPC emergence

To gain further support for a role of Gpr183-Arrb1-Notch1 cascade during the differentiation of HSPCs from HECs, we asked if 7 α -25-OHC treatment would facilitate the generation of HSPCs. Both *runx1* mRNA level and protein level were significantly upregulated in 7 α -25-OHC-treated embryos (Figure 5D and 5E). Moreover, the frequency of cells undergoing EHT in Tg(*flk1*:mCherry/*cmyb*:GFP) embryos was markedly increased after 7 α -25-OHC treatment (Supplementary information, Movie S2). These results support the notion that the activated Gpr183-Arrb1-Notch1 cascade facilitates HSPC

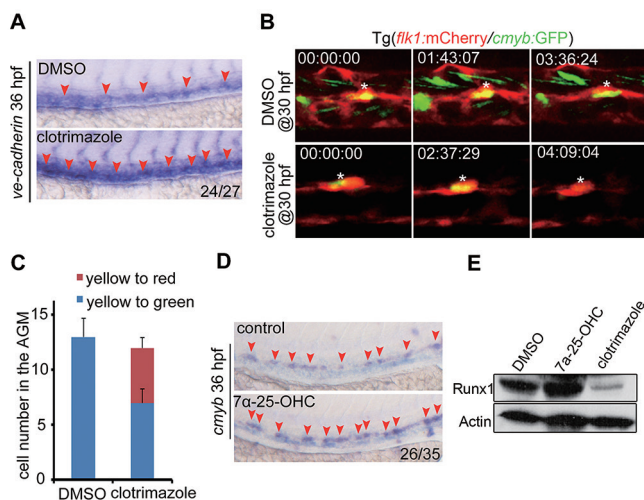


Figure 5 7α -25-OHC stimulation facilitates HSPC development in zebrafish. **(A)** Expression of *ve-cadherin* increases in clotrimazole-treated embryos. **(B)** Transition of HE to HSPCs or non-hemogenic ECs after DMSO or clotrimazole treatment beginning at 30 hpf. White asterisk indicates the same cell in different frames. **(C)** Quantification of HE ($flk1^+cmyb^+$, yellow cells in **B**) differentiating to HSPCs ($flk1^-cmyb^+$, green cells in **B**) or non-hemogenic ECs ($flk1^+cmyb^-$, red cells in **B**) ($n = 5$). Error bar represents SD. **(D, E)** *runx1* expression in embryos treated with 7α -25-OHC or clotrimazole and examined at 36 hpf by WISH **(D)** and western blotting **(E)**. Red arrowheads in **A** and **D** label the staining signals in AGM.

emergence *in vivo*.

Regulation of HSPC emergence by *Gpr183* is conserved in mammals

We next asked whether the regulation of HSPC emergence by *gpr183* is conserved in mammals. Among three populations sorted from the AGM region of E11 mice: non-hemogenic EC ($c\text{-Kit}^-CD31^+CD41^-CD45^-Ter119^-$), HEC ($c\text{-Kit}^+CD31^+CD41^-CD45^-Ter119^-$) and HSPC ($c\text{-Kit}^+CD34^+$), HE had the greatest level of *gpr183* expression, consistent with the results in zebrafish (Figure 6A). Expression levels of *ch25h* and *cyp7b1* in the mouse AGM region increased markedly from E10.5 to E11.5 (Figure 6B), and these enzymes were highly enriched in non-hemogenic ECs ($c\text{-Kit}^+CD31^+CD41^-CD45^-Ter119^-$) (Supplementary information, Figure S7B). Moreover, the colony forming ability of cells isolated from AGM was significantly reduced after clotrimazole treatment in a colony forming unit in spleen (CFU-S) assay (Figure 6C–6E), confirming the role of *Gpr183* in hematopoiesis. To examine directly whether *gpr183* regulates EHT, pan-ECs ($CD31^+CD41^-CD45^-Ter119^-$) were sorted from the E10 caudal half and cultured with clotrimazole (Figure

6F) [34]. Remarkably, clotrimazole treatment reduced HSPC population ($CD45^+c\text{-Kit}^+$) [34] in a dose-dependent manner in OP9 co-cultures (Figure 6G and 6H), indicating that ablation of *gpr183* signaling suppresses HSPC development. To determine whether *gpr183* signaling specifically affects HE, we sorted non-hemogenic ECs, HECs or HSPCs from the E11 AGM region and treated them with clotrimazole. As shown in Supplementary information, Figure S7C, only HECs displayed a significant decreased hematopoietic capability, supporting that *gpr183* signaling specifically targets HECs but not non-hemogenic ECs and HSPCs. To further determine whether *gpr183* signaling contributes to the emergence of HSPCs, we conducted a long-term transplantation assay, in which cells dissected from AGM region of E11 embryo ($CD45.1/2$) were treated with DMSO or clotrimazole and then transplanted into irradiated mice ($CD45.2$; Figure 6F). Four months after the transplantation, all 6 recipients were successfully repopulated with DMSO-treated cells, with a donor chimerism in bone marrow ranging from 30% to 80% (Figure 6I). Multiple hematopoietic lineages derived from the donor cells were detected in peripheral blood of recipients (Figure 6J). The donor cells also displayed a potent self-renewal capacity upon transplantation into secondary recipients (Figure 6K–6L). In contrast, the AGM cells treated with clotrimazole failed to reconstitute any recipients (Figure 6I; 0/6, 2 independent experiments), suggesting that HSPC development was disrupted upon *Gpr183* signaling deficiency. Taken together, we conclude that *Gpr183* signaling is a conserved regulatory mechanism during HSPC emergence in vertebrates.

The *Gpr183*-*Arrb1*-*Notch1* signaling cascade is conserved in mammals

To determine whether *Gpr183*-*Arrb1* represses *Notch1* expression in mammals, we dissected cells from E10.5 mouse AGM region and treated them with either 7α -25-OHC or clotrimazole. Both *Notch1* and *NICD* expression levels were decreased after 7α -25-OHC stimulation, but increased after clotrimazole treatment (Figure 7A and 7B). We next performed immunoprecipitation (IP) assay using anti-*Arrb1* with cells dissected from E10.5 mouse AGM region and found that after 7α -25-OHC stimulation, both *Gpr183* and *Notch1*, as well as the E3 ligase *Nedd4*, were precipitated by anti-*Arrb1* (Figure 7C). Interestingly, *Gpr183* was precipitated by an antibody against *Notch1* even in the absence of 7α -25-OHC stimulation (Figure 7C), indicating that *Gpr183* is localized adjacent to *Notch1* and serves as an important switch to downregulate the *Notch1* level before the onset of HSPC emergence. Moreover, consistent with results shown in

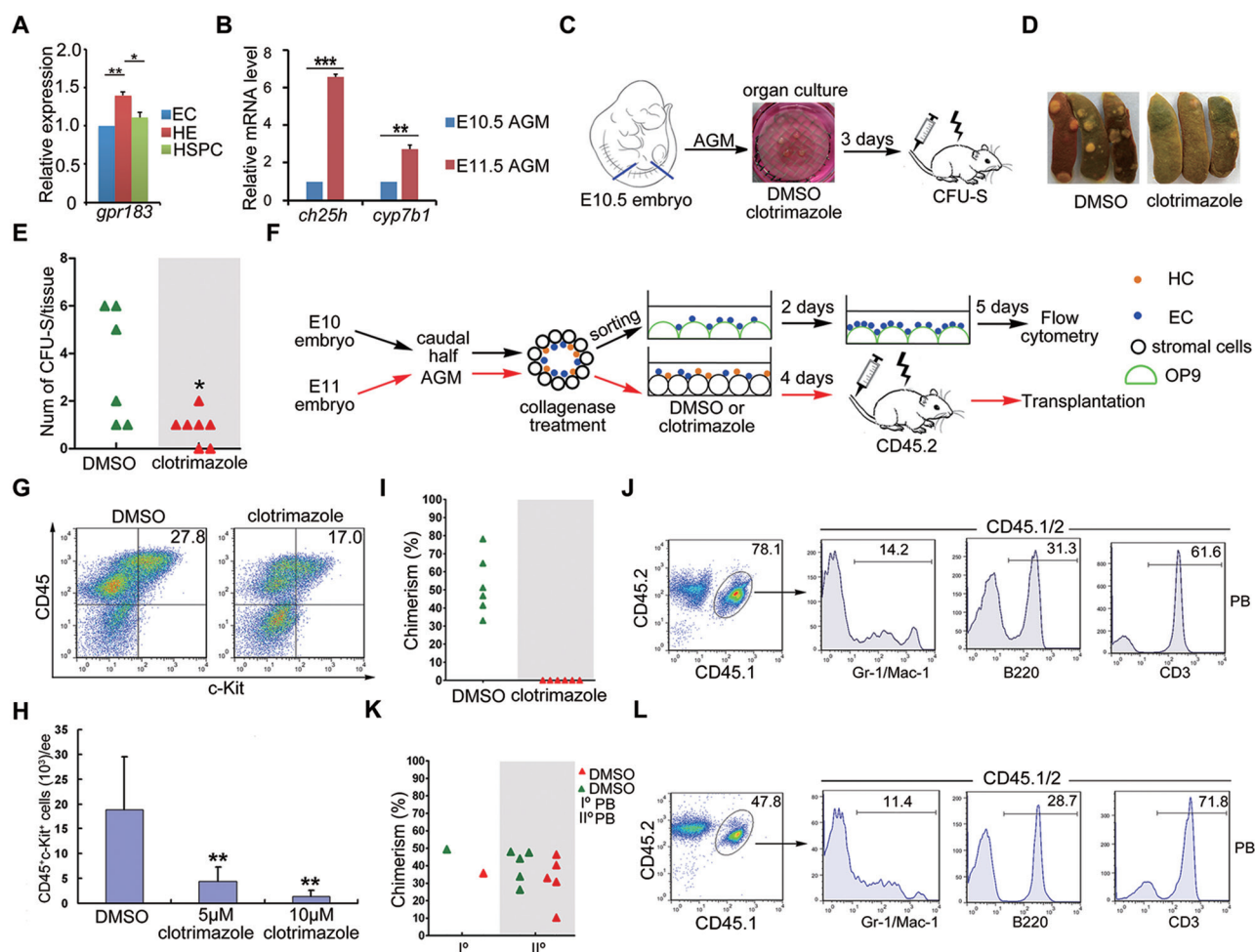


Figure 6 *Gpr183* function during HSPC development is conserved in mammals. **(A)** *gpr183* expression by RT-PCR in non-hemogenic ECs, HECs and HSPCs sorted from the AGM region of E11 mouse embryos. **(B)** Expression of *ch25h* and *cyp7b1* in mouse AGM region (E10.5 and E11.5; $n = 3$ for each time point). **(C)** Flowchart of CFU-S assay. **(D, E)** CFU-S colony number is significantly reduced in mice transplanted with clotrimazole-treated cells. **(F)** Schematic illustration of flow cytometry analysis and long-term transplantation in mouse. E10 mouse caudal half and E11 mouse AGM region were dissected and dissociated by collagenase. Pan-ECs (CD31⁺CD41⁻CD45⁺Ter119⁻) from E10 caudal half were sorted and cultured with DMSO or clotrimazole before flow cytometry analysis. AGM cells from E11 mouse (CD45.1/2) embryos (but not sorted pan-ECs as they often resulted in poor reconstitution) were treated with DMSO or clotrimazole for 4 days and transplanted into irradiated C57BL/6J (CD45.2) mice. HC, hematopoietic cells; EC, pan-ECs; OP9, feeder cells used in co-culture. **(G, H)** Representative FACS plots **(G)** and quantification **(H)** of CD45⁺c-Kit⁺ HSPCs from OP9 co-cultures. **(I)** Donor-derived chimerism in recipients. Each symbol represents the percentage of donor chimerism in bone marrow of a recipient 4 months post-transplantation. **(J)** Multiple hematopoietic lineages including myeloid (Gr1⁺/Mac-1⁺), B lymphoid (B220⁺), and T lymphoid (CD3⁺) populations in peripheral blood of the recipients (CD45.2) transplanted with E11 AGM cells (CD45.1/2) pre-treated with DMSO. **(K, L)** Donor-derived chimerism **(K)** and multi-lineage potential **(L)** in peripheral blood of secondary recipients (II^o) transplanted with bone marrow cells of repopulated primary recipients (I^o). Symbols in **K** represent the donor chimerism in peripheral blood of individual secondary recipients 12 weeks post-transplantation. Symbols of same color indicate the donor and the related secondary recipients. Data are presented as mean \pm SD. * $P < 0.05$, ** $P < 0.01$, *** $P < 0.001$.

Figure 4D, MG132 treatment rescued the reduction of NICD protein levels induced by 7α -25-OHC stimulation in mouse AGM cells (Figure 7D). Taken together, we conclude that activated *Gpr183* recruits *Arb1* and E3 ligase *Nedd4* to degrade *Notch1* through the ubiquitin-pro-

teasome pathway in mouse.

In Tie2-positive endothelial cells, *Notch1* expression level was decreased after 7α -25-OHC treatment (Supplementary information, Figure S7D and S7E). Pan-ECs (CD31⁺CD41⁻CD45⁺Ter119⁻) from the E11 mouse

AGM generated markedly more HSPCs in the presence of 7 α -25-OHC (Figure 7E and 7F). Furthermore, 7 α -25-OHC treatment promoted the production of functional HSPCs *in vivo* in a CFU-S assay (Figure 7E and 7G). In addition, 7 α -25-OHC treatment promoted the rate of chimerism in recipients in a three-month transplantation assay (Figure 7H, Supplementary information, Figure S7F and S7G). These results, together with the data obtained in zebrafish, demonstrate the conservation of Gpr183-Arrb1-Notch1 signaling cascade as an essential regulatory mechanism for the development of HSPCs in vertebrates (Supplementary information, Figure S8).

Discussion

It is well known that HSPCs are generated from specified HE in AGM, but the mechanism governing this process remains poorly understood. The EHT involves cell shape changes, cell migration and cell-cell communication [5-7], and is regulated by a complex network of cell-intrinsic and cell-extrinsic signals. Exploring the signals that induce EHT is of great importance for our understanding of HSPC development and may provide insights into clinical applications in regenerative medicine. Our genome-wide transcriptome analyses of non-homogenic ECs, HECs, and HSPCs reveal that *gpr183* begins to be highly expressed in HECs, and is downregulated in HSPCs. Functional analysis demonstrates that Gpr183, upon activation by its endogenous ligand 7 α -25-OHC, specifically modulates HSPC development through repressing Notch1 signaling. An unexpected finding is that Notch1 signaling is not continuously required for HSPC development, and persistent activation of Notch1 signaling after HE specification abrogates EHT, suggesting a temporally restricted role of Notch1 during HSPC development. Moreover, our results show that 7 α -25-OHC-activated Gpr183 signaling is a conserved signaling mechanism regulating HSPC development.

RNA-Seq using a Tg(runx1:en-GFP) line identifies an important regulator of HSPC emergence

Our newly generated *runx1:en-GFP* transgenic line, with robust and specific fluorescence signals, has been proved recently to be capable of labeling functional HSPCs [22]. High-throughput RNA-Seq using this transgenic line in current study uncovers significant transcriptome variations among non-homogenic ECs, specified HECs and HSPCs during HSPC development in zebrafish. Moreover, GO analysis identifies various GPCRs that are enriched in ECs, HECs or HSPCs. Based on our results and several previous findings [19, 20, 35], we postulate that multiple GPCRs influence HSPC develop-

ment through complex mechanisms that are still poorly understood. Gpr183 was previously reported to guide immune cell migration [23, 24]. Our current work assigns a new role for Gpr183 during embryonic HSPC development based on the observations that blocking Gpr183 signaling significantly attenuates HSPC generation, while activating Gpr183 leads to more functional HSPCs. Similar results obtained from two animal models, zebrafish and mouse, indicate Gpr183 is a conserved and essential regulator of HSPC emergence in vertebrates.

After HE specification, continuous Notch signaling inhibits HSPC development

Recent studies using pluripotent stem cells (PSCs) in *in vitro* culture systems have indicated that Notch signaling is essential for the generation of functional HSPCs [33, 36]. However, a previous study using mouse AGM-derived cell lines as feeder cells to support the differentiation of hematopoietic cells from human embryonic stem cells has also reported that downregulation of Notch signaling facilitates the production of hematopoietic cells [37]. Based on previous studies on Notch signaling during HSPC development and our results here, we speculate that HSPC development is intricately regulated and *in vitro* culture systems might not properly recapitulate the endogenous signaling processes. Our work supports that Notch signaling is not continuously required for HSPC development. Blocking Notch signaling before HE specification nearly completely disrupts HSPC generation, consistent with previous findings [11]; however, after HE specification, persistent Notch signaling can convert HECs into non-homogenic ECs, thus abrogating subsequent HSPC development. The temporal regulation of HSPC development by a specific signaling pathway is not rare. For instance, Wnt signaling is essential for HE specification, but has to be downregulated to allow HSPC development to proceed further [38, 39]. These findings together imply the complexity of mechanisms governing HSPC development, and each signaling pathway essential for hematopoiesis must be tightly regulated at different developmental stages.

Gpr183 downregulates Notch1 through Nedd4-mediated ubiquitination

Our work reveals that activated Gpr183 recruits Arrb1 and Nedd4 to degrade Notch1 through the ubiquitination-proteasome process, and this Gpr183-Arrb1-Nedd4-Notch1 signaling cascade is evolutionarily conserved in both zebrafish and mouse. The contribution of Arrb1 and Nedd4 to HSPC development has not been reported before, although Arrb1 is known to regulate primitive hematopoiesis by relieving PcG-mediated repression of

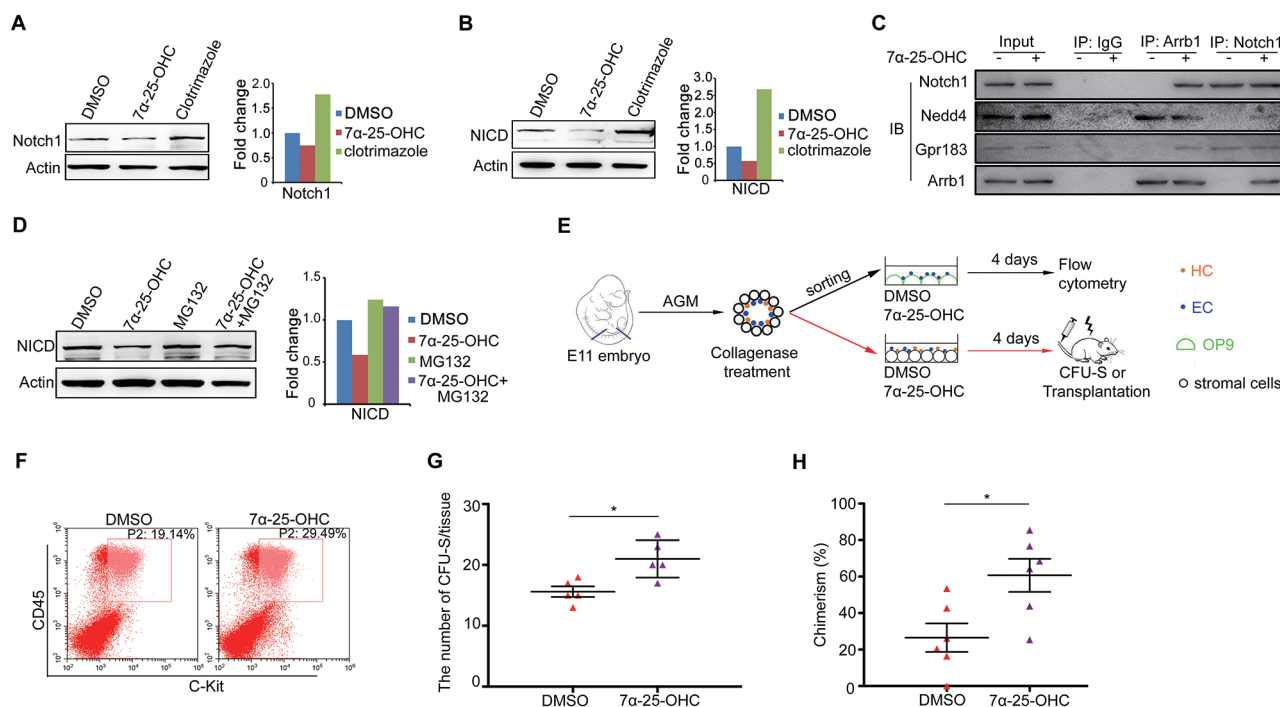


Figure 7 Gpr183-Arrb1-Notch1 signaling cascade is conserved in mammals. **(A, B)** Notch1 and NICD expression in E10.5 mouse AGM cells treated with clotrimazole or 7 α -25-OHC for 1 h. **(C)** Western blot detection of Gpr183 or Notch1 in anti-Arrb1 or anti-Notch1 IP product from E10.5 AGM cells. Equal amounts of Notch1 were used in the co-IP assay as 7 α -25-OHC treatment decreases Notch1 expression and thus it is difficult to detect Notch1-precipitated proteins in the IP assay. **(D)** Decrease in NICD expression in 7 α -25-OHC-treated E10.5 AGM cells is rescued by MG132. Right panel shows the quantification of western blot data. **(E)** Flowchart for isolation, culture and transplantation of mouse AGM cells. For flow cytometry, pan-ECs (CD31⁺CD41⁻CD45⁺Ter119⁻) were sorted from cell suspension obtained from E11 mouse AGMs and treated with DMSO or 7 α -25-OHC for 4 days. For CFU-S or long-term transplantation assay, total E11 AGM cells were treated with DMSO or 7 α -25-OHC for 4 days. **(F)** Flow cytometry showing an increased amount of c-Kit⁺CD45⁺ cells from 7 α -25-OHC-treated E11 mouse AGM pan-ECs. **(G)** Quantification of results from the CFU-S assay ($n = 5$). **(H)** Donor-derived chimerism. AGM cells from actin-GFP transgenic mice were treated with DMSO or 7 α -25-OHC (1 μ M) for 4 days, mixed with bone marrow carrier cells, and were injected intravenously into irradiated female mice (GFP⁻). Three months later, bone marrow cells were collected for the analysis of GFP⁺ chimerism. Error bar represents SD. * $P < 0.05$.

cdx4-hox signaling [40]. Here we show that disruption of each component in the Gpr183-Arrb1-Nedd4-Notch1 cascade leads to a HSPC differentiation defect, highlighting the importance of this signaling pathway during HSPC development. A recent study has indicated that the HECT family E3 ligase Itch inhibits homeostasis of the bone marrow HSPCs by degrading Notch1 [41]. However, we did not detect an enriched expression of Itch in our MS dataset. *In vitro* ubiquitination assay further confirms that Itch is not involved in Notch1 ubiquitination in embryonic HSPCs (data not shown).

What remains to be clarified is how Notch1 in HE inhibits EHT. Based on our results we speculate that the specified HE possess both hemogenic and endothelial properties held in a fine balance, and an elevation in the Notch1 protein level, similar to the enhanced ERK signaling as we reported before [42], is able to strengthen

the arterial cells identity [16], resulting in a loss of hematopoietic marker expression accompanied by an increase of adhesion molecule expression, and an aborted EHT.

7 α -25-OHC serves as a potent agonist of HSPC emergence

Expression of Ch25h and Cyp7b1 is enriched in endothelial cells in the AGM region of both zebrafish (data now shown) and mouse, suggesting that 7 α -25-OHC derived from the HSPC niche activates Gpr183 through a paracrine mechanism. Here, we find that Gpr183 serves as a switch to abrogate Notch1 activity after 7 α -25-OHC stimulation, indicating that specified HE receive signals from the surrounding niche to trigger EHT. 7 α -25-OHC-stimulated Gpr183 signaling facilitates HSPC development, which is reminiscent of recent findings that small molecules, such as PGE2 and epoxye-

icosatrienoic acids (EETs), can serve as GPCR ligands to facilitate HSPC differentiation or expansion [19, 43]. The mechanisms of their action are emerging. EETs promote HSPC development in zebrafish embryos through an unknown GPCR that activates AP-1, which in turn upregulates *runx1* expression in both AGM and CHT in zebrafish embryos. In addition, EETs also efficiently enhance HSPC homing and engraftment in mammals [43]. These findings and ours demonstrate that GPCR signaling pathways are evolutionarily conserved important regulators of HSPC development and function, and their ligands may have clinical applications in blood transplantation and regenerative medicine.

Materials and Methods

Zebrafish

Zebrafish strains including Tubingen, Tg(*runx1:en-GFP*), Tg(*flk1:mCherry/runx1:en-GFP*), Tg(*flk1:mCherry/cmyb:GFP*), Tg(*tp1:mCherry*) [44], Tg(*fli1a:eGFP/tp1:mCherry*), Tg(*scl:a:dsRed*) [45], Tg(*rag2:dsRed*) (provided by Zilong Wen), Tg(*hsp70:dn-MAML*) [29], Tg(*hsp70:Gal4*) [30], Tg(*UAS:NICD*) [30] and *gpr183* heterozygous mutant, were raised in the experimental animal center in the Institute of Zoology, Chinese Academy of Science. Embryos were staged according to the number of somites. For imaging, embryos were raised in the presence of 0.003% 1-phenyl-2-thiourea to avoid pigment formation. *gpr183*^{-/-} was generated in *AB/Tuebingen* background. This study was approved by the Ethical Review Committee of the Institute of Zoology, Chinese Academy of Sciences, China.

Morpholinos, mRNA synthesis, qPCR, western blotting, BrdU/TUNEL assay, and double fluorescence in situ hybridization (dFISH)

All morpholinos were purchased from GeneTools and are listed in Supplementary information, Table S4 along with the dosages used in this study. mRNA synthesis, qPCR, western blotting, BrdU/TUNEL assay, and dFISH were performed as previously described [46, 47]. qPCR primers are listed in Supplementary information, Table S5. For the *Gpr183*-GFP internalization experiment, *gpr183*-eGFP and *arrb1*-mCherry mRNA were co-injected into one-cell stage embryos. At about 90% epiboly, embryos were dechlorinated and incubated with Hoechst for 30 min, and treated with DMSO or 7 α -25-OHC (1 μ M, Sigma, SML0541) for 10 min. Embryos were crushed by cover glass for observation.

Cell sorting and RNA-deep sequencing

The trunk region of 28 hpf Tg(*flk1:mCherry/runx1:en-GFP*) embryos was dissected and dissociated into single cells as previously described [48]. mCherry⁺GFP⁻, mCherry⁺GFP⁺, mCherry⁻GFP⁺ cells were sorted using BD FACS Aria I. 1 ng of total RNA extracted using QIAGEN RNeasy Micro kit was reversely transcribed and amplified as previously described [49]. cDNA samples were sequenced using Illumina HiSeq2500 to produce 101 bp paired-end sequence reads. Quality of raw RNA-seq reads for each sample was controlled by FastQC software and bases with quality scores less than 20 were removed by Trimmomatic. The remaining reads were mapped to the Zebrafish reference cDNA sequences

(zv9, from Ensembl) by BWA. .

Differentially expressed genes between two groups were determined using the R-package DESeq2, with criterion *P* value cutoff of 0.001 and fold change cutoff of 2. Heatmap was generated by R-package Heatmap2 according to RPKMs (reads per kilobase per million reads) of each gene in multiple samples. The RNA-Seq dataset is shown in Supplementary information, Table S1.

Cell transfection and co-IP assay

Zebrafish *gpr183* and *arrb1* coding sequences were ligated into the pCMV-Flag and pcDNA4ToMycHisB plasmids, respectively. According to the Lipo2000 (Invitrogen) transfection protocol, the plasmids were transfected into 293T cells for the co-IP assay. 24 h later, cells were treated with 1 μ M 7 α -25-OHC for 0.5 h before harvesting. Proteins were purified in RIPA buffer (50 mM Tris, 150 mM NaCl, 10% Glycerol, 5 mM MgCl₂, 0.5% NP40, and Roche cocktail protease inhibitor) and mixed with anti-c-Myc agarose affinity gel antibody (Sigma, A7470). 3-4 h later, beads were collected for western blotting. Antibodies used were anti-c-Myc (Sigma, M4439, 1:2 000) and anti-Flag (Sigma, F7425, 1:1 000).

Zebrafish confocal imaging

Embryos for microscopic observation and photography were prepared as previously described [50]. Supplementary information, Movie S1 was captured using ZEISS LSM 510 confocal microscopy. Supplementary information, Movie S2 and fluorescent images were taken using Nikon A1 confocal microscopy. Supplementary information, Movies S3 and S4 were captured using Perkin Elmer spinning disk confocal microscopy.

Chemical treatment

Zebrafish embryos at 10 somite stage (14 hpf) or 26 hpf were treated with clotrimazole (10 μ M; Sigma, C6019) or DBZ (8 μ M; Sigma, SML0649). 7 α -25-OHC (4.2 pg) was injected into one-cell stage embryos. Embryos were treated with MG132 (10 μ M, Sigma C2211) from 26 to 36 hpf.

Mice

Mice were kept at the Animal Center of the Academy of Military Medical Sciences according to institutional guidelines. Embryos were staged by somite number: E10, 31-40 sp, and E11, 41-50 sp. This study was approved by the Ethical Review Committee of the Academy of Military Medical Sciences, China.

Mouse co-IP assay and western blotting

E10.5 mouse AGM regions were dissected and dissociated into single cell suspension using 0.1% collagenase. After a 3-day culture in the presence of hematopoietic cytokines (50 ng/ml SCF, 50 ng/ml IL-3, and 20 ng/ml FLT3), cells were starved for 4 h and pretreated with MG132 (10 μ M, Sigma C2211) for 2 h, and then treated with 7 α -25-OHC for 0.5 h (or 1 h in Figure 4F) before harvesting. Cells were lysed in RIPA buffer (50 mM Tris, 150 mM NaCl, 10% Glycerol, 5 mM MgCl₂, 0.5% NP40, and Roche cocktail protease inhibitor), and incubated with Arrb1 (Abcam, ab32097, 1:100) or Notch1 (Abcam, ab65297, 1:100) antibody for 4 h at 4 °C. Protein A agarose (Invitrogen, 15918014) was added next to the mixture which was incubated for another 3-4 h. Beads were collected for western blotting using following antibodies: β -actin (cell signaling, 4967, 1:2000), Notch1 (Abcam, ab128076, 1:1 000), Notch1 (Abcam, ab65297, 1:1 000), NICD (Abcam,

ab83232, 1:500), Gpr183 (Abcam, ab168744, 1:1 000), Arrb1 (Abcam, ab32097, 1:5 000), and ubiquitin (Santa Cruz, sc8017, 1:1 000).

Mass spectrometry

E10.5 mouse AGM was dissected and dissociated into single cells, which were cultured for three days in the presence of hematopoietic cytokine, before being treated with either DMSO or 7 α -25-OHC for 1 h. Anti-Notch1 (Abcam, ab65297, 1:100) was used for the IP. LTQ Orbitrap Elite was used to perform the MS. The entire dataset is shown in Supplementary information, Tables S2 and S3.

Protein purification

His-Ubc4, His-Ub, RGS-H-flag-NICD, GST-Ub E1, GST-Nedd4 and other Ub E3 ligases were first affinity purified, then fractionated by size exclusion chromatography on Superdex75 and Superdex200 column in a reaction buffer containing 50 mM Tris-HCl, pH 8.0, 150 mM KCl, 5% glycerol and 2 mM MgCl.

In vitro ubiquitination assay

Ubiquitination experiment was carried out as follows: 60 nM E1, 300 nM Ubc4 (E2), 300 nM Nedd4 (E3) and 500 nM NICD were incubated with 1 μ M ubiquitin at 30°C in a reaction buffer containing 25 mM Tris-HCl, pH 7.4, 2 mM MgCl/ATP, and 0.2 mM DTT. Samples were collected 2 h later, and were mixed with the Laemmli buffer in the presence of a reducing reagent for western blotting.

GST Pull-down

Nedd4-GST was incubated with GST beads at 4 °C for 2 h (GST protein was used as a negative control). The beads were centrifuged and washed in NP40 buffer (50 mM Tris-HCl, pH 8.0, 150 mM NaCl and 0.5% NP40) three times. RGS-FLAG-NICD was added to the mixture, which was incubated for additional 2 h at 4 °C. Following the incubation, the beads were centrifuged and washed 3 times in NP40 buffer, before a loading buffer was added. The samples were heated at 65 °C for 5 min and analyzed by western blotting.

AGM explant and CFU-S assay

Mouse AGMs were dissected and cultured as explants for 3 days as previously described [51]. In brief, AGMs were deposited on nylon filters (Millipore) placed on metallic supports and cultured in a medium for myeloid long-term culture (Stem Cell Technologies) supplemented with 10 μ M hydrocortisone (Stem Cell Technologies). To this air-liquid interphase culture we added either DMSO, or 1 μ M 7 α -25-OHC, or 10 μ M clotrimazole. The AGMs after treatment were dissociated by 0.04% collagenase for 40 min at 37 °C. Cells were injected intravenously into female C57BL/6J mice that had been exposed to a split dose of 9 Gy γ -irradiation (⁶⁰Co, 4.5 + 4.5 Gy with 2 h interval). After 11 days, animals were sacrificed and their spleens were removed and fixed in Bouin's fixative. Spleen colonies were counted under a dissecting microscope.

OP9 co-cultures

FACS-sorted CD31⁺CD41⁻CD45⁻Ter119⁻ pan-ECs from E10 caudal half were cultured on OP9 stromal cells in the presence of

cytokines (100 ng/ml SCF, 100 ng/ml IL-3, and 100 ng/ml FLT3), and were treated with DMSO, 1 μ M 7 α -25-OHC or 10 μ M clotrimazole for 2 days. After additional 5 days of co-culture, cells were harvested by trituration using a pipet for subsequent flow cytometry analysis.

Long-term transplantation assay

Male C57BL/6J (CD45.2) and female C57BL/6J (CD45.1) mice were mated to obtain CD45.1/2 embryos. The AGMs of E11 (43-45 sp) embryos were digested in 0.1% collagenase for 30 min at 37 °C. Individual cells were cultured in the presence of DMSO or 10 μ M clotrimazole plus hematopoietic cytokines (100 ng/ml SCF, 100 ng/ml IL-3, and 100 ng/ml FLT3). After 4 days of culture, cells were harvested by pipetting and enzymatic digestion. These cells, together with 2 \times 10⁴ bone marrow carrier cells (CD45.2), were injected intravenously into irradiated female C57BL/6J mice (CD45.2). Chimerism in peripheral blood and bone marrow was measured 16 weeks after the transplantation. To examine the self-renewal potential, secondary transplantation was performed, in which a total of 3 \times 10⁶ cells from the bone marrow of a primary recipient were intravenously injected into a secondary recipient. Donor-derived chimerism was assessed by flow cytometry using anti-CD45.2-PE and anti-CD45.1-APC antibodies (eBioscience) 12 weeks after transplantation. Mice demonstrating over 10% donor-derived chimerism (contributing to both myeloid and lymphoid lineages) after a minimum of 12 weeks were considered to be reconstituted. The contribution of transplanted cells to the different lineages was measured by flow cytometry with specific antibodies against CD3, B220, Mac1, Gr1, CD4 and CD8 (eBioscience). For transplantation of 7 α -25-OHC-treated cells, 0.3 embryo-equivalent donor cells from actin-GFP transgenic C57BL/6J mice were treated with DMSO or 1 μ M 7 α -25-OHC, mixed with 2 \times 10⁴ bone marrow cells (GFP⁻), and injected intravenously into irradiated female mice (GFP⁻). Three months later, bone marrow cells were analyzed for GFP⁺ chimerism.

Statistical analysis

All experiments were repeated at least three times, except for the long-term transplantation after clotrimazole treatment. Student's two-tailed *t*-test was used for statistical analysis.

Acknowledgments

We thank Elaine Dzierzak and David Traver for helpful discussions and critical reading of the paper. We thank Baofa Sun and Yungui Yang for bioinformatics analysis, Anming Meng, Zilong Wen and Jing-Wei Xiong for providing reagents used in this work. This work was supported by the National Basic Research Program of China (2010CB945300 and 2011CB943900), the National Natural Science Foundation of China (31271570 and 31425016), and the Strategic Priority Research Program of the CAS (XDA01010110).

References

- 1 Dieterlen-Lievre F. Hematopoiesis: progenitors and their genetic program. *Curr Biol* 1998; **8**:R727- R730.
- 2 Jaffredo T, Nottingham W, Liddiard K, Bollerot K, Pouget C, de Bruijn M. From hemangioblast to hematopoietic stem cell:

- an endothelial connection? *Exp Hematol* 2005; **33**:1029-1040.
- 3 Medvinsky A, Rybtsov S, Taoudi S. Embryonic origin of the adult hematopoietic system: advances and questions. *Development*, 2011; **138**:1017-1031.
 - 4 Kaimakis P, Crisan M, Dzierzak E. The biochemistry of hematopoietic stem cell development. *Biochim Biophys Acta* 2013; **1830**:2395-2403.
 - 5 Kissa K, Herbomel P. Blood stem cells emerge from aortic endothelium by a novel type of cell transition. *Nature* 2010; **464**:112-115.
 - 6 Bertrand JY, Chi NC, Santoso B, Teng S, Stainier DY, Traver D. Haematopoietic stem cells derive directly from aortic endothelium during development. *Nature* 2010; **464**:108-111.
 - 7 Boisset JC, van Cappellen W, Andrieu-Soler C, Galjart N, Dzierzak E, Robin C. *In vivo* imaging of haematopoietic cells emerging from the mouse aortic endothelium. *Nature* 2010; **464**:116-120.
 - 8 Zhang CR, Patient R, Liu F. Hematopoietic stem cell development and regulatory signaling in zebrafish. *Biochim Biophys Acta* 2013; **1830**:2370-2374.
 - 9 Clements WK, Traver D. Signalling pathways that control vertebrate haematopoietic stem cell specification. *Nat Rev Immunol* 2013; **13**:336-348.
 - 10 Orkin SH, Zon LI. Hematopoiesis: an evolving paradigm for stem cell biology. *Cell* 2008; **132**:631-644.
 - 11 Burns CE, Traver D, Mayhall E, Shepard JL, Zon LI. Hematopoietic stem cell fate is established by the Notch-Runx pathway. *Genes Dev* 2005; **19**:2331-2342.
 - 12 Zhong TP, Childs S, Leu JP, Fishman MC. Gridlock signaling pathway fashions the first embryonic artery. *Nature* 2001; **414**:216-220.
 - 13 Lawson ND, Vogel AM, Weinstein BM. Sonic hedgehog and vascular endothelial growth factor act upstream of the Notch pathway during arterial endothelial differentiation. *Dev Cell* 2002; **3**:127-136.
 - 14 Robert-Moreno A, Guiu J, Ruiz-Herguido C, et al. Impaired embryonic haematopoiesis yet normal arterial development in the absence of the Notch ligand Jagged1. *EMBO J* 2008; **27**:1886-1895.
 - 15 Richard C, Drevon C, Canto PY, et al. Endothelial-mesenchymal interaction controls runx1 expression and modulates the notch pathway to initiate aortic hematopoiesis. *Dev Cell* 2013; **24**:600-611.
 - 16 Lizama CO, Hawkins JS, Schmitt CE, et al. Repression of arterial genes in hemogenic endothelium is sufficient for hematopoietic fate acquisition. *Nat Commun* 2015; **6**:7739.
 - 17 Wettschreck N, Offermanns S. Mammalian G proteins and their cell type specific functions. *Physiol Rev* 2005; **85**:1159-1204.
 - 18 Yue R, Li H, Liu H, et al. Thrombin receptor regulates hematopoiesis and endothelial-to-hematopoietic transition. *Dev Cell* 2012; **22**:1092-2100.
 - 19 North TE, Goessling W, Walkley CR, et al. Prostaglandin E2 regulates vertebrate hematopoietic stem cell homeostasis. *Nature* 2007; **447**:1007-1011.
 - 20 Solaimani Kartalaei P, Yamada-Inagawa T, Vink CS, et al. Whole-transcriptome analysis of endothelial to hematopoietic stem cell transition reveals a requirement for Gpr56 in HSC generation. *J Exp Med* 2015; **212**:93-106.
 - 21 Ng CE, Yokomizo T, Yamashita N, et al. A Runx1 intronic enhancer marks hemogenic endothelial cells and hematopoietic stem cells. *Stem Cell* 2010; **28**:1869-1881.
 - 22 Tamplin OJ, Durand EM, Carr LA, et al. Hematopoietic stem cell arrival triggers dynamic remodeling of the perivascular niche. *Cell* 2015; **160**:241-252.
 - 23 Hannedouche S, Zhang J, Yi T, et al. Oxysterols direct immune cell migration via EBI2. *Nature* 2011; **475**:524-527.
 - 24 Liu C, Yang XV, Wu J, et al. Oxysterols direct B-cell migration through EBI2. *Nature* 2011; **475**:519-523.
 - 25 Heinig M, Petretto E, Wallace C, et al. A trans-acting locus regulates an anti-viral expression network and type 1 diabetes risk. *Nature* 2010; **467**:460-464.
 - 26 Rose KA, Stapleton G, Dott K, et al. Cyp7b, a novel brain cytochrome P450, catalyzes the synthesis of neurosteroids 7alpha-hydroxy dehydroepiandrosterone and 7alpha-hydroxy pregnenolone. *Proc Natl Acad Sci USA* 1997; **94**:4925-4930.
 - 27 Lund EG, Kerr TA, Sakai J, Li WP, Russell DW. cDNA Cloning of mouse and human cholesterol 25-hydroxylases, polytopic membrane proteins that synthesize a potent oxysterol regulator of lipid metabolism. *J Biol Chem* 1998; **273**:34316-34327.
 - 28 Tang Y, Bai H, Urs S, Wang Z, Liaw L. Notch1 activation in embryonic VE-cadherin populations selectively blocks hematopoietic stem cell generation and fetal liver hematopoiesis. *Transgenic Res* 2013; **22**:403-410.
 - 29 Zhao L, Borikova AL, Ben-Yair R, et al. Notch signaling regulates cardiomyocyte proliferation during zebrafish heart regeneration. *Proc Natl Acad Sci USA* 2014; **111**:1403-1408.
 - 30 Scheer N, Campos-Ortega JA. Use of the Gal4-UAS technique for targeted gene expression in the zebrafish. *Mech Dev* 1999; **80**:153-158.
 - 31 Lefkowitz RJ, Whalen EJ. beta-arrestins: traffic cops of cell signaling. *Curr Opin Cell Biol* 2004; **16**:162-168.
 - 32 Kim AD, Melick CH, Clements WK, et al. Discrete Notch signaling requirements in the specification of hematopoietic stem cells. *EMBO J* 2014; **33**:2363-2373.
 - 33 Ditadi A, Sturgeon CM, Tober J, et al. Human definitive hemogenic endothelium and arterial vascular endothelium represent distinct lineages. *Nat Cell Biol* 2015; **17**:580-591.
 - 34 Li Z, Lan Y, He W, et al. Mouse embryonic head as a site for hematopoietic stem cell development. *Cell Stem Cell* 2012; **11**:663-675.
 - 35 Yue R, Li H, Liu H, et al. Thrombin receptor regulates hematopoiesis and endothelial-to-hematopoietic transition. *Dev Cell* 2012; **22**:1092-1100.
 - 36 Gori JL, Butler JM, Chan YY, et al. Vascular niche promotes hematopoietic multipotent progenitor formation from pluripotent stem cells. *J Clin Invest* 2015; **125**:1243-1254.
 - 37 Huang C, Jackson M, Samuel K, Taylor AH, Lowell S, Forrester LM. Haematopoietic differentiation is inhibited when Notch activity is enhanced in FLK1(+) mesoderm progenitors. *Stem Cell Res* 2013; **11**:1273-1287.
 - 38 Chanda B, Ditadi A, Iscove NN, Keller G. Retinoic acid signaling is essential for embryonic hematopoietic stem cell development. *Cell* 2013; **155**:215-227.
 - 39 Ruiz-Herguido C, Guiu J, D'Altri T, et al. Hematopoietic stem cell development requires transient Wnt/beta-catenin activity. *J Exp Med* 2012; **209**:1457-1468.

- 40 Yue R, Kang J, Zhao C, *et al.* Beta-arrestin1 regulates zebrafish hematopoiesis through binding to YY1 and relieving polycomb group repression. *Cell* 2009; **139**:535-546.
- 41 Rathinam C, Matesic LE, Flavell RA. The E3 ligase Itch is a negative regulator of the homeostasis and function of hematopoietic stem cells. *Nat Immunol* 2011; **12**:399-407.
- 42 Zhang C, Lv J, He Q, *et al.* Inhibition of endothelial ERK signalling by Smad1/5 is essential for haematopoietic stem cell emergence. *Nat Commun* 2014; **5**:3431.
- 43 Li P, Lahvic JL, Binder V, *et al.* Epoxyeicosatrienoic acids enhance embryonic haematopoiesis and adult marrow engraftment. *Nature* 2015; **523**:468-471.
- 44 Parsons MJ, Pisharath H, Yusuff S, *et al.* Notch-responsive cells initiate the secondary transition in larval zebrafish pancreas. *Mech Dev* 2009; **126**:898-912.
- 45 Zhen F, Lan Y, Yan B, *et al.* Hemogenic endothelium specification and hematopoietic stem cell maintenance employ distinct Scl isoforms. *Development* 2013; **140**:3977-3985.
- 46 Wang L, Liu T, Xu L, *et al.* Fev regulates hematopoietic stem cell development via ERK signaling. *Blood* 2013; **122**:367-375.
- 47 Wei Y, Ma D, Gao Y, Zhang C, Wang L, Liu F. Ncor2 is required for hematopoietic stem cell emergence by inhibiting Fos signaling in zebrafish. *Blood* 2014; **124**:1578-1585.
- 48 Covassin L, Amigo JD, Suzuki K, Teplyuk V, Straubhaar J, Lawson ND. Global analysis of hematopoietic and vascular endothelial gene expression by tissue specific microarray profiling in zebrafish. *Dev Biol* 2006; **299**:551-562.
- 49 Tang F, Barbacioru C, Nordman E, *et al.* RNA-Seq analysis to capture the transcriptome landscape of a single cell. *Nat Protoc* 2010; **5**:516-535.
- 50 Renaud O, Herbomel P, Kissa K. Studying cell behavior in whole zebrafish embryos by confocal live imaging: application to hematopoietic stem cells. *Nat Protoc* 2011; **6**:1897-1904.
- 51 Medvinsky A, Dzierzak E. Definitive hematopoiesis is autonomously initiated by the AGM region. *Cell* 1996; **86**:897-906.

(Supplementary information is linked to the online version of the paper on the *Cell Research* website.)



This license allows readers to copy, distribute and transmit the Contribution as long as it attributed back to the author. Readers are permitted to alter, transform or build upon the Contribution as long as the resulting work is then distributed under this is a similar license. Readers are not permitted to use the Contribution for commercial purposes. Please read the full license for further details at - <http://creativecommons.org/licenses/by-nc-sa/4.0/>